Engineering Structures 198 (2019) 109463

Contents lists available at ScienceDirect

Engineering Structures

journal homepage: www.elsevier.com/locate/engstruct

Weight estimation on static B-WIM algorithms: A comparative study

Felipe Carraro*, Matheus Silva Gonçalves, Rafael Holdorf Lopez, Leandro Fleck Fadel Miguel, Amir Mattar Valente

Laboratório de Transportes e Logística (LabTrans) and Center for Optimization and Reliability in Engineering (CORE), Civil Engineering Department, Federal University of Santa Catarina, Rua João Pio Duarte Silva, s/n, 88040-900 Florianópolis, SC, Brazil

ARTICLE INFO

Keywords:
Bridge weigh-in-motion
Vehicle weight prediction
Methods comparison
Inverse problems
Statistical assumptions

ABSTRACT

Bridge weigh in motion (B-WIM) comprises the use of sensors on existing bridges in order to assess the loads of passing vehicles. Although numerous methods for weight estimation on static B-WIM algorithms may be found in the literature, there is not available a comparison study among them, especially regarding accuracy and statistical assumptions. Hence, this paper provides a critical comparison on a subset of conceptually similar B-WIM methods, further extending the discussion on their theoretical assumptions, beyond what is currently available in literature. The methods are not only referenced but reinterpreted and reformulated in a unifying manner, allowing an in-depth comparison. Moreover, a parametric study on the performance and sensitivity of methods is conducted. Not only simulated but also real data are employed in the comparison, supporting conclusions.

1. Introduction

A bridge weigh in motion (B-WIM) system effectively turns a bridge in a weighing mechanism by means of recovering the live load of passing vehicles from strain information obtained through sensors. These systems are installed underneath the bridge, which does not disrupt road traffic and also improves the durability and portability of the system [1]. Therefore, it can be an efficient tool for overweight enforcement since it is able to measure vehicles weight traveling at operating speed. The information retrieved from the system can also be employed in other contexts such as maintenance planning, structural health monitoring, service life estimation and traffic network planning [2]. The cost of installing and maintaining B-WIM systems is therefore often lower due to better accessibility and synergy effects with other projects when compared to other traffic monitoring systems [3].

The main idea behind B-WIM systems, firstly introduced by Moses [4], relies on equating the bending moment on the bridge with the product of the magnitude of the applied moving load and the influence line ordinate of the bridge. By this formulation, it is possible to estimate the axle weights of passing vehicles as those which generate the best agreement between theoretical and measured bending moment response. For more aspects regarding general information about B-WIM systems, as well as some implementation considerations, the reader is referred to Lydon et al. [5], Yu et al. [6], Žnidarič et al. [7].

Differently from the theoretical influence line employed by Moses, recently developed approaches apply crossing vehicles with known weight and the corresponding measured deformations to derive the influence line of the bridge, a procedure known as calibration [8–11]. This formulation is valid as long as the static analysis is considered. In practice, however, the dynamical motions induced by vehicles may increase the difficulty in the correct influence line evaluation and consequently weight prediction [12].

Due to the dynamic behavior, B-WIM methods may be divided into two classes, related to explicitly considering or not the dynamic formulation and bridge-vehicle interaction. Several papers contributed with different approaches in the first class, with a higher emphasis on the concept of Moving Force Identification (MFI) [13–15,1,12,16]. This class of methods, however, may need to consider a full 3D model of the bridge for a suitable accuracy, thus requiring extensive computational effort [6]. Therefore, although some promising results, MFI methods are not yet able to deal with some important applications, such as real-time monitoring [17]. For the static class, which is the focus of this paper, several researchers presented novel contributions in the past decade. Ieng [8] proposed a maximum likelihood approach to estimate the bridge influence line, generalizing the method by simultaneously taking into account measurements available from as many calibration trucks as needed. Zhao et al. [9] considered the transverse distribution of wheel loads on the axle weight estimation. Kim et al. [18] trained artificial neural networks for the estimation of Gross Vehicle Weights (GVW). O'Brien et al. [10] introduced the concept of probabilistic

* Corresponding author.
E-mail addresses: felipecarraro@gmail.com (F. Carraro), matheusgoncalves.contato@gmail.com (M.S. Gonçalves), rafael.holdorf@ufsc.br (R.H. Lopez), leandro.miguel@ufsc.br (L.F.F. Miguel), amir.valente@ufsc.br (A.M. Valente).

https://doi.org/10.1016/j.engstruct.2019.109463
Received 20 December 2018; Received in revised form 6 July 2019; Accepted 30 July 2019
Available online 08 August 2019

influence line seeking to find the most probable axle weights. O'Brien et al. [11] employed Tikhonov regularization for overcoming the ill-posedness of the B-WIM problem.

Although the performance of proposed methods is usually argued as useful for practical application, their results often disregard other recent studies in the same subject. As a consequence, it becomes hard to evaluate the state-of-the-art improvements, since each study relies on specific bridges, whose performance are not directly comparable with each other. Furthermore, although some of those methods make direct statistical assumptions, similarities with other approaches and practical consequences of these assumptions are usually not evaluated. Indeed, there has not been identified any publications comparing theoretical aspects, practical applicability as well as the performance of recent B-WIM algorithms.

In the present work, a comparative investigation, comprised of 5 state-of-the-art methods on weight estimation using static B-WIM algorithms, is conducted. The methods employed in this investigation are presented in Ieng [8], Zhao et al. [9], O'Brien et al. [10], O'Brien et al. [19] and O'Brien et al. [11], which are related to influence line acquisition, weight prediction or both simultaneously. In the proposed analysis, all methods are reformulated or reinterpreted in a unified manner, allowing theoretical statistical comparisons. Furthermore, the practical consequences of some assumptions are discussed.

In order to perform the proposed analysis, a large set of distinct conditions, such as bridge span and road profile, is numerically simulated. The generated data set is employed for improving comparisons, since it enables relating the bridge properties and a method's performance. It may help users in choosing the most suitable method for their specific case. Furthermore, real-world signals are also evaluated, offering validation for the conclusions drawn based on the simulated model.

The main contribution of this paper is to conduct an investigation of B-WIM procedures, further explaining their theoretical considerations, the relation among methods and presenting a comparison of their performance. The methods are not only discussed as referenced, but are reinterpreted and reformulated in a unifying manner, employing a similar notation, which more easily enables comparisons. Thus, the analyses pursued here aim to lead to new insights for the development of novel methods or for choosing methods based on which cases they are likely to perform better.

The paper is organized as follows: Section 2 employs the same formulation framework on the analyzed methods, enabling not only numerical but conceptual, theoretical and implementation comparisons. Section 3 presents the numerical comparison of all methods using simulated data, and remarking some theoretically expected aspects. The results obtained from real field data are presented in Section 4. Finally, Section 5 addresses further comments and discussion while Section 6 presents concluding remarks.

2. Methods overview and discussion

General aspects regarding the methods that belong to the scope of this study are discussed in this section. Further analyses are conducted for five methods whose characteristics are relevant for the overall comparative context. For the remaining methods, the aspects that prevent their inclusion in the comparative study are remarked.

2.1. Matrix method

The study of O'Brien et al. [19] develops the matrix method for the acquisition of the influence line. It derives the equations for three-axle calibration trucks by minimizing a quadratic residual based on the predicted response of a pre-weighted vehicle. In their study, the influence line for two vehicles with three and seven axles are calibrated and the similarity between measured and predicted responses is shown. This work contributed with a systematic way of employing direct bridge measurements by first calibrating an influence line based on a pre-weighted truck, which is later used for weighing arbitrary vehicles. This contrasts with the use of the theoretical influence line proposed in Moses [4].

2.1.1. The Matrix approach itself

The Matrix method results in a least squares solution. The basic idea starts from Moses algorithm, where one must minimize an error function R, comprised of the sum of the squares of differences between the measured bending moment M^m and the theoretical bending moment M^t. The measured term, for an instant k is given by:

$$M_k^m = \sum_{g=1}^{G} E_g Z_g \varepsilon_g, \tag{1}$$

where G represent the number of girders and E_g, Z_g, and ε_g are the elastic modulus, section modulus and measured strain of the $g-th$ girder, respectively. The theoretical term introduces the influence line and reads:

$$M_k^t = \sum_{j=1}^{J} W_j IL_{(k-Cj)}, \tag{2}$$

where

$$C_j = \frac{d_j f}{v} \tag{3}$$

and J is the number of axles, W_j is the weight of the $j-th$ axle, $IL_{(k-Cj)}$ is the influence ordinate at the position of the $j-th$ axle, d_j is the distance between the first axle and $j-th$ axle, C_j is the number of scans corresponding to d_j, f is the sampling frequency and v is the vehicle velocity. It is worthwhile to point that if $k-C_j$ results in a index that does not match an influence line ordinate, it is attributed the value of zero for it.

The error term reads:

$$R = \sum_{k=1}^{K} (M_k^m - M_k^t)^2, \tag{4}$$

where k represent each scan and K the total number of scans. Differently from the work of Moses, where M^t was based on a theoretical influence line, in O'Brien et al. [19] it is now considered an unknown and solved with the minimization of Eq. (4) by calibrating with a vehicle with known weight. After the influence line based on direct measurements has been found, one can proceed as usual with Moses method for finding the unknown weights of vehicles passing over the bridge. That is:

$$W = (\Lambda^T \Lambda)^{-1} \Lambda^T M^m \tag{5}$$

where W is the vector of predicted axle weights and Λ is a matrix based on the influence line ordinates, shifted according to the axle spacing, defined as:

$$\Lambda^{kj} = IL_{k-C_j}. \tag{6}$$

Thus, Λ is a $K \times J$ matrix. Furthermore, the same observation done for IL_{k-C_j} in Eq. (2) holds here.

The error function in Eq. (4) defines a least square problem. By the statistical point of view, such an approach is the maximum likelihood estimator when errors are independent and normally distributed random variables [20]. These errors are related to each measured ordinate and at the same event of calibration. However, these underlying error assumptions may not be met when considering practical cases. For example, missing information on formulation could be seen as correlated errors [21]. Thus, if the model description in Eq. (2) is not accurate enough, a least squares estimate would not provide the best result. Nevertheless, one could still extract useful information from the method application, even though minor violations on the assumptions are present [22].

2.2. The maximum likelihood approach

The work of Ieng [8] proposes the utilization of maximum likelihood estimation (MLE) to obtain the influence line, based on calibration data. The main reason argued by the study is that the method proposed by O'Brien et al. [19] is not robust enough and the influence line derivation is done only with signals produced by a single pass of the calibration vehicle. Thus, the MLE approach intended to overcome these issues, applying an iid (independent and identically distributed) Gaussian random noise to the formulation.

Ieng [8] compared the MLE approach with the matrix method of O'Brien et al. [19], using the L_∞ norm (maximum value of error) between predicted and measured strains as the criterion. The presented results were derived using different traffic data from the one employed in calibration. Ieng [8] concluded that the applied methodology achieved smaller errors regarding to the measured strains.

2.2.1. The MLE approach itself

Measurements are always corrupted with some kind of noise, introducing uncertainties into the analysis. The maximum likelihood approach aims to include these uncertainties into the formulation in order to reach a more robust influence line.

It is assumed in MLE that the measurements are corrupted by ϵ, a zero mean multivariate normal random variable:

$$M^m = M^t + \epsilon, \tag{7}$$

where M^m and M^t are the vectors of measured and modeled moments, respectively, such that:

$$M^t = AIL, \tag{8}$$

where IL is a vector with the ordinates of the influence line and A is a Toeplitz matrix of the loads. The matrix A is based on the impulse load vector $\mathscr{W}$:

$$\mathscr{W}_i = \begin{cases} W_j, & \text{if } i = C_j + 1 \\ 0, & \text{otherwise} \end{cases}, \tag{9}$$

where W_j is the weight of the $j-th$ axle and C_j is analogous to that one defined in Eq. (3). This impulse vector represents the whole vehicle, with each axle load at their respective axle position. The A matrix is formed by shifting $\mathscr{W}$ in each line of A, which corresponds to a discrete convolution, where each line relates to a time step of the vehicle passing over the bridge:

$$A = \begin{bmatrix} W_1 & \dots & 0 & \dots & 0 \\ \vdots & \ddots & \vdots & \ddots & \vdots \\ W_J & \dots & W_1 & \dots & 0 \\ \vdots & \ddots & \vdots & \ddots & \vdots \\ 0 & \dots & W_J & \dots & W_1 \\ \vdots & \ddots & \vdots & \ddots & \vdots \\ 0 & \dots & 0 & \dots & W_J \end{bmatrix}_{(K \times K - Cj)}, \tag{10}$$

where K and J are the total number of scans and axles, respectively.

Furthermore, several calibration trucks could be employed, passing N times over the bridge. Each passage of the vehicle could be counted as a realization of the random variable ϵ. Then, the notation may be modified to:

$$M_i^m = M_i^t + \epsilon_i, \tag{11}$$

where the index i ranges from 1 to N, the total number of signals collected. In order to merge data from distinct runs, one could suppose that all data collected is related to the same random variable. In this way, it becomes necessary to interpolate the data vectors to common ordinates.

Assuming that the realizations of this variable are independent among events, the likelihood can be written as the product of the individual probabilities:

$$L = \prod_{i=1}^{N} \text{pdf}(\epsilon_i | IL), \tag{12}$$

where pdf is the probability density function of ϵ and L is the likelihood. The principle of MLE is equivalent to minimizing the negative of its natural logarithm with respect to IL:

$$\text{argmax}_{IL}\left(\prod_{i=1}^{N} \text{pdf}(\epsilon_i | IL)\right) = \text{argmin}_{IL}\left(-\sum_{i=1}^{N} (\log(\text{pdf}(\epsilon_i | IL)))\right). \tag{13}$$

Inserting Eq. (11) into Eq. (13), it reads:

$$\text{argmin}_{IL}\left(-\sum_{i=1}^{N} (\log(\text{pdf}(M_i^m - M_i^t | IL)))\right). \tag{14}$$

As the variable ϵ follows a multivariate normal distribution, the expression of its pdf could be introduced into the formulation:

$$\text{argmin}_{IL}\left(-\sum_{i=1}^{N} \log\left(\frac{1}{|\Sigma|\sqrt{(2\pi)^K}} \exp^{-\frac{1}{2}((M_i^m - AIL)^T \Sigma^{-1} (M_i^m - AIL))}\right)\right), \tag{15}$$

where Σ is the covariance matrix of the random variable ϵ, $|.|$ is the determinant operator and K is the number of dimensions of the multivariate distribution, which corresponds to the number of scans in this case. Using the logarithm properties:

$$\text{argmin}_{IL}\left(\sum_{i=1}^{N} \left(\log(|\Sigma|\sqrt{(2\pi)^K}) + \frac{1}{2}(M_i^m - AIL)^T \Sigma^{-1} (M_i^m - AIL)\right)\right). \tag{16}$$

This expression can be minimized by setting to zero its first derivative with respect to IL. Supposing that the covariance matrix Σ is independent of the IL ordinates, it results that the derivative of the first term is zero. The derivative of the remaining expression can be written as:

$$\sum_{i=1}^{N} \frac{1}{2} \frac{\partial}{\partial IL_j} ((M_i^m - AIL)^T \Sigma^{-1} (M_i^m - AIL)) = 0, \tag{17}$$

which results in:

$$\sum_{i=1}^{N} ((M_i^m - AIL)^T \Sigma^{-1} A) = 0. \tag{18}$$

Recalling that $(AB)^T = B^T A^T$ and Σ is a symmetric matrix:

$$\sum_{i=1}^{N} (A^T \Sigma^{-1} (M_i^m - AIL))^T = 0. \tag{19}$$

Rearranging the expression and assuming that the covariance is a diagonal matrix, with equal variance:

$$\sum_{i=1}^{N} A^T AIL = \sum_{i=1}^{N} A^T M_i^m, \tag{20}$$

the expression proposed in the study is reached. To find the solution it is necessary for $\sum_{i=1}^{N} A_i^T A_i$ to be invertible, condition that is satisfied according to Ieng [8]. Similarly to the work of O'Brien et al. [19], the MLE method provides a way to find the influence line based on calibration data. Thus, the weighing procedure is also analogous to that stated by Moses.

2.2.2. Comparing MLE and matrix method

The comparative aspect between MLE and matrix method was already assessed in the work of Ieng [8]. The matrix method was derived based on data of only one calibration run, while the MLE approach could be seen as a generalization of the matrix method for cases where more calibration runs were performed. Hence, the matrix method needs some kind of assembly strategy, such as performing the mean of resulting influence lines from several runs. It is worthwhile mentioning

that, as previously discussed for the matrix method, the MLE approach will only be the maximum likelihood estimator when errors are independent and normally distributed random variables, with equal standard deviation.

2.3. pBWIM

The pBWIM approach was proposed by O'Brien et al. [10], which aimed to directly incorporate probabilistic information about several passages of calibration vehicles to construct the influence line. This formulation assumed that each measured influence line ordinate follows a normal distribution, obtained from field testing. The matrix method is employed to derive the parameters of these distributions, based on a single influence line for each event. Finally, the estimated axle weights are those with the highest probability of occurrence among all possible combinations.

In order to derive the pBWIM results, two different levels of information were applied to generate the influence line: the whole calibration data or only a subset of events. The goal was to reproduce a situation closer to the real case, whose small number of calibration events are available. The results showed that with less information, the pBWIM achieved better results in comparison with the traditional approach.

2.3.1. The pBWIM approach itself

Considering that the response M^t is the sum of products of axle weights and influence line ordinates, the response related to scan k, M_k^t, could be written as:

$$M_k^t = \sum_{j=1}^{J} W_j IL_{k-C_j}, \tag{21}$$

where J is the number of axles, W is the vector of axle weights, IL_{k-C_j} is the influence line value at ordinate $k - C_j$ and C_j is the offset distance between the ordinates of the influence line related to axle j. If the value of $k - C_j$ results in an index that does not correspond to an influence line ordinate, the value zero is attributed to it, since it reflects a situation where the axle is out of the bridge.

Since each influence line ordinate follows a known normal distribution and the response M_k^t is a linear combination of normal variables, the response M_k^t itself also follows a normal distribution. Thus, each ordinate has a corresponding normal distribution defined by the parameters:

$$\mu_k^M = \sum_{j=1}^{J} W_j \mu_{k-C_j} \tag{22}$$

$$\sigma_k^M = \sqrt{\sum_{j=1}^{J} \left(W_j \sigma_{k-C_j}\right)^2 + \tau^2}, \tag{23}$$

where μ_k^M and σ_k^M are the mean and standard deviation of the random variable related to the predicted moment of each bridge ordinate k, respectively. Furthermore, τ and σ_{k-C_j} are the standard deviation of the measurement noise and influence line, respectively.

Given the measured moments M_k^m, related to a specific bridge ordinate, the probability of a set of weights being responsible for generating such measures could be formulated as (highlighting those terms that rely on the weights W):

$$P_k(W) = \frac{1}{\sigma_k^M(W)\sqrt{2\pi}} \exp\left(-\frac{1}{2}\left(\frac{M_k^m - \mu_k^M(W)}{\sigma_k^M(W)}\right)^2\right). \tag{24}$$

Assuming that all random variables related to the measured moments on each ordinate are independent, an expression for finding the weights that most likely have generated such data could be formulated as:

$$\text{argmax}_W\left(\prod_{k=1}^{K} P_k(W)\right), \tag{25}$$

where K is the total number of scans in the measured response. Therefore, it is necessary to find the weights that maximize this expression. The procedure described by O'Brien et al. [10] to obtain the axle weights is based on a grid search, whose bounds and increments are arbitrary parameters. Such study has applied 0.8 and 1.2 times the weights predicted by the matrix method as bounds and 0.1 kN as increment. It is worth pointing that such a procedure is quite time-consuming, especially when increasing the number of axles.

2.3.2. The assumption of independence

Although pBWIM method provided reasonable results, an assumption made in the derivation of the procedure seems to be violated. In order to better understand it, one can write the response M^t in matrix formulation, as already discussed in Eq. (8):

$$M^t = AIL, \tag{26}$$

where A is the Toeplitz matrix for a given set of axle loads and IL is the influence line vector, assumed to be comprised by independent Gaussian random variables by O'Brien et al. [10]. As IL is supposed to be Gaussian, it is straightforward to calculate the covariance matrix of the resulting moments random vector M^t, dealing with A as a linear transformation applied to the IL random variables:

$$\Sigma_{M^t} = A^T \Sigma_{IL} A, \tag{27}$$

where Σ_{M^t} and Σ_{IL} are the covariance matrix of the predicted moments and influence line, respectively. Recalling that Σ_{IL} is diagonal, since the influence line ordinates are defined as independent random variables, and writing the matrix multiplication with index notation, results in an expression for each term of the Σ_{M^t} matrix:

$$\Sigma_{M^t}^{ij} = \sum_{k=1}^{K} A_{ik} \Sigma_{IL}^{kk} A_{jk}, \tag{28}$$

where K is the total number of scans. As already mentioned, for the predicted moments to be independent random variables, it is necessary that Σ_{M^t} be diagonal. Matematically, for all i and j, with $i \neq j$, one must have $\Sigma_{M^t}^{ij} = 0$. Thus, for showing that such independence does not occur, it is enough that there are i and j, with $i \neq j$, such that $\Sigma_{M^t}^{ij} \neq 0$.

Observing Eq. (28), it could be noticed that A_{ik}, A_{jk} and Σ_{IL}^{kk} will always be non-negative. The first two because of the structure of matrix A, which is comprised only by axles weights and zeros, as seen in Eq. (10). The last one is strictly greater than zero, since it is the diagonal of a covariance matrix. Therefore, just one term of the summation greater than zero is sufficient to ensure a non-diagonal covariance. In other words, it is enough that, for any k, there are i and j, with $i \neq j$, such that:

$$A_{ik} A_{jk} > 0. \tag{29}$$

One could see that the condition of Eq. (29) is always met when, at least, one column in A has more than one non-negative value. For the Toeplitz matrix A, it occurs when the passing vehicle has more than one axle, being the difference between the corresponding i and j equal to the number of scans separating both axles. Thus, for the general case, Σ_{M^t} is not a diagonal matrix and predicted moments are not independent random variables, violating this assumption. It is worth to mention that if the matrix A is diagonal, which corresponds to a vehicle with only one axle passing over the bridge, the independence holds. However, such a case is clearly unrepresentative for B-WIM applications.

2.3.3. Comparing pBWIM and MLE approaches

In the definition of the pBWIM approach, O'Brien et al. [10] account for a zero mean error in the measurement. In this way, the stated formulation could be seen as a total least squares, with the form:

$$(IL + \epsilon)W = M^m + \tau, \tag{30}$$

where IL now is a matrix containing the influence line ordinates in each column, shifted by the corresponding axle spacing in the rows and W is the vector of weights. However, as it became necessary to have some estimate for the standard deviation of the measurement noise, O'Brien et al. [10] set this value to zero. Therefore, resulting in a problem such that:

$$(IL + \epsilon)W = M. \tag{31}$$

Such a formulation remarks the difference between pBWIM and MLE approaches. The former accounts for error in the independent variable while the latter sums it to the dependent variable. While the formulation of MLE results in a closed-form solution, the approach of pBWIM requires some form of optimization procedure in order to find the most likely weights. Furthermore, pBWIM does not make any assumption regarding errors with equal standard deviation, which is the case for MLE.

2.4. Tikhonov regularization

O'Brien et al. [11] applied Tikhonov regularization to the matrix method equations. The reason is that the final system of equations used to solve the axle weights has an ill-conditioned or ill-posed nature. With this approach, the authors intended to achieve better results mainly for the weight by axle, which is acknowledged to have worse prediction precision than total vehicle weight. The author used the well known L curve method [23] to define the regularization parameter, evaluating parameters ranging from 10^{-90} to 600,000. It is worth to mention that the solution is unique for each parameter.

The method was theoretically tested using dynamic simulations of a series of moving forces on a bridge. The author concluded that the regularized solution performed better than the matrix method. However, as the vehicle dynamics increased, the convergence of the regularized solution was not as accurate.

2.4.1. The Tikhonov regularization approach itself

Tikhonov or ridge regression is a regularization technique that uses the least squares framework with the addition of another term that depends on a regularization parameter λ. This term can be viewed as a penalization aimed at improving the conditioning of the system. One can employ the colon notation to denote the Frobenius inner product and Frobenius norm, respectively:

$$A: B = \mathrm{tr}(A^T B), \tag{32}$$

$$\|A\|_F^2 = \mathrm{tr}(A^T A) = A: A, \tag{33}$$

and consider the error function of the full matrix case:

$$R = M^m - TW, \tag{34}$$

where M^m represents measured moments, W are axle weights and T is a matrix used to perform the convolution procedure between influence line and weights.

In Tikhonov regularization, one should minimize a function f, comprising the error norm as well as the regularized solution norm, with respect to the matrix W. Therefore, writing function f as:

$$f = \|R\|_F^2 + \lambda\|W\|_F^2 = R: R + \lambda W: W, \tag{35}$$

it is straightforward to compute the differential and gradient as follows:

$$\begin{aligned} df &= 2R: dR + 2\lambda W: dW \\ &= 2(M - TW): -T dW + 2\lambda W: dW \\ &= 2T^T(TW - M): dW + 2\lambda W: dW \\ &= (2T^T(TW - M) + 2\lambda W): dW \end{aligned} \tag{36}$$

$$\frac{\partial f}{\partial W} = 2T^T(TW - M) + 2\lambda W. \tag{37}$$

Setting this gradient to zero, one can find an expression for the optimal weight matrix:

$$\begin{aligned} 2T^T(TW - M) + 2\lambda W &= 0 \\ T^T TW - T^T M + \lambda W &= 0 \\ (T^T T + \lambda I)W &= T^T M \\ W &= (T^T T + \lambda I)^{-1} T^T M, \end{aligned} \tag{38}$$

where the matrix I represents the identity matrix.

Considering that each λ parameter defines a unique regularized solution W_λ, the nontrivial task is to obtain the optimal regularization parameter for the problem solution. Numerous methods exist for this task such as cross-validation [24], ridge trace [25], and the L-curve method [26]. In their study, O'Brien et al. [11] opts for the L-curve method where two norms are defined. The first one is the residual norm of the error for each specific regularization parameter, given by:

$$E_{norm} = \sqrt{(M - TW_\lambda)^T (M - TW_\lambda)}. \tag{39}$$

The second, is the norm of the solution for each regularization parameter, given by:

$$F_{norm} = \sqrt{W_\lambda^T W_\lambda}. \tag{40}$$

According to the method, the optimal λ is located at the corner of the curve constructed by plotting F_{norm} and E_{norm} on a log-log scale. The corner, represents a trade-off between bias and variance on the system approximation. Fig. 1 illustrates the usual shape of the L-curve. O'Brien et al. [11] does not details the process of optimal lambda selection. Nevertheless, other regularization parameters could be obtained given different approaches for finding the L-curve corner such as the Spline-based Curvature Method [27], Triangle Method [28] or Adaptive Pruning [29]. Considering that the numerous algorithms focused only on the L-curve approach exist, which often returns different "optimal" points, the task of finding the optimal regularization parameter is seen as complex and subjective [10].

2.4.2. Statistical aspects behind the regularization approach

In order to understand the statistical interpretation of the formulation employed by O'Brien et al. [11], we make use of the analogy of Bayesian methods and regularization where the maximum a priori estimate of a normal prior with normal likelihood results in the same estimation as a Tikhonov regularization (for demonstration and proof the reader is referred to Aster et al. [20]). That is, by the Bayesian perspective, initial probability statements are updated, providing a posterior distribution that combines both prior knowledge and the data

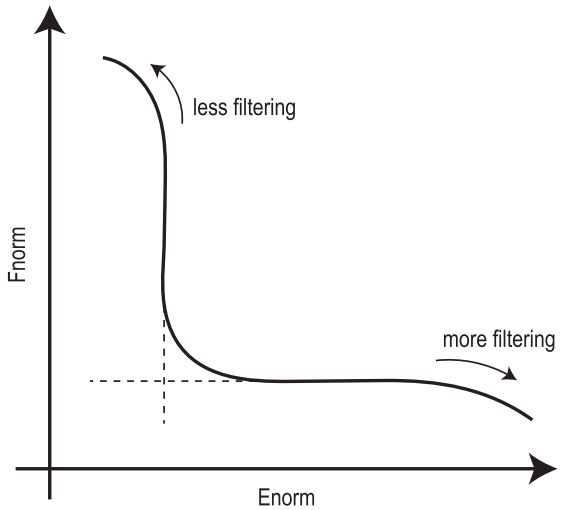

Fig. 1. The generic form of the L-curve plotted in double-logarithmic scale, adapted from: [23].

at hand [30]. Thus, instead of a single estimate as output, Bayesian statistics provide a probability distribution for the model parameters. It is worthwhile mentioning that it is possible to derive a single estimate from such posterior as, for instance, its maximum *a posteriori* (MAP). The prior distribution is obtained independently of the results of measurements [31]. It could represent in a B-WIM application, for example, the knowledge about the non-negativity of predicted axle weights.

The regularization procedure could be interpreted from a Bayesian perspective. The MAP solution obtained by using a prior with independent and normally distributed model parameters is precisely the Tikhonov regularized solution, as demonstrated in Aster et al. [20]. Aligning this interpretation with the already discussed aspect of a trade-off between bias and variance, the regularization parameter arises as the ratio between noise and prior variances [32]. Thus, a lower regularization parameter means a less informative prior is adopted. For the extreme case of zero in the regularization parameter, the least square solution is obtained.

However, Tikhonov regularization and Bayesian approach are not entirely equivalent, since Bayesian solution is a probability distribution, while the Tikhonov solution is a single set of parameters [20]. Hence, the regularization procedure could be seen as a bridge between non-Bayesian and Bayesian estimation problems [32].

When employing Bayesian or regularization approaches, some bias is introduced to the formulation. Accordingly to the adopted method, straightforward ways for incorporating each kind of prior knowledge could be reached. However, the formulation developed by O'Brien et al. [11] has not made use of any prior information as, for example, the already discussed non-negativity of axle weights. Thus, making use of such knowledge could result in improved weigh procedures, for both regularization and Bayesian approaches.

2.5. Including transverse position into formulation

The work of Zhao et al. [9] accounts for the transverse distribution of axle loads on each girder in the formulation. By using the calculated influence line of each girder as a reference, a modified 2D Matrix method was derived to identify axle weights of moving vehicles. Zhao et al. [9] emphasized that, although there are theoretical approximations for the transverse load distribution, the measured data was employed to generate one transverse distribution coefficient for each girder.

The results presented are based on two calibration vehicles, passing 10 times on each lane. Therefore, the influence line of each girder is the mean of each event. Zhao et al. [9] concluded that the method is suitable for simply supported concrete slab-girder bridges. It is noteworthy that the study did not compare the results with the matrix method, or any other method. Finally, some limitations are cited at the end of the paper, such as that the methodology is not suitable for box-girder bridges or other long-span bridge forms.

2.5.1. The modified 2D Matrix method itself

An additional parameter Q_g is introduced into the model of the 2D modified method. It is supposed to represent the transverse distribution of the vehicle loads on each girder. Zhao et al. [9] calculated it based on the 50 largest strains, as the ratio between the strain of a given girder and the total value:

$$Q_g = \frac{\varepsilon_{g,k}}{\sum_{g=1}^{G} \varepsilon_{g,k}}, \tag{41}$$

where k is a scan related to one of the 50 largest strains and $\varepsilon_{g,k}$ is the strain measured for scan k and girder g, of a total of G girders. Thus, this measure can be seen as the percentage of total strain that distributes on each girder. Although the study recognizes that along the driving direction the transverse load distribution factor of each girder is position-dependent, a constant value for each girder was applied. The reason is that most slab-girder bridges have equally distributed lateral connectivity in the vicinity of the mid-span. Furthermore, it supposes that, after calculating the contribution of each girder, each one is responsible for their own load only, independent of the others.

The algorithm for influence line calculation is analogous to the Matrix method, however resulting in one influence line per girder. It is based on a least-squares minimization of the difference between the measured and predicted strains at mid-span:

$$R_g = \sum_{k=1}^{K} (\varepsilon_{g,k}^m - \varepsilon_{g,k}^t)^2, \tag{42}$$

where $\varepsilon_{g,k}^m$ and $\varepsilon_{g,k}^t$ are the measured and predicted strains at scan k and girder g. Furthermore, R_g is the squared error, calculated individually for each girder g. The predicted strain could be written as:

$$\varepsilon_{g,k}^t = \frac{1}{E_g Z_g} \sum_{j=1}^{J} W_j Q_g I_{g,(k-C_j)} \tag{43}$$

where $W_j Q_g$ is the weight contribution of the $j-th$ axle on each girder.

Using the matrix notation applied for all methods analyzed here, the influence line for each girder could be calculated as:

$$IL_g = ((AQ_g)^T (AQ_g))^{-1} (AQ_g)^T E_g Z_g \varepsilon_g^m, \tag{44}$$

where IL_g is the vector of influence line ordinates for the girder g, A is Toeplitz matrix of loads described in Eq. (10).

The weighing procedure is based on a least square minimization between predicted and measured moments, considering the axle weights as variables of interest. In order to maintain consistency with the previous formulation, the weighing procedure may be written as:

$$W = ((\Lambda_Q)^T \Lambda_Q)^{-1} \Lambda_Q \sum_{g=1}^{G} (E_g Z_g \varepsilon_g^m) \tag{45}$$

$$= ((\Lambda_Q)^T \Lambda_Q)^{-1} \Lambda_Q M^m, \tag{46}$$

where Λ_Q is a matrix of influence line ordinates defined by:

$$\Lambda_Q = IL_G \times_n Q^T, \tag{47}$$

where Q is the vector grouping the transverse distribution parameters of all girders, $\times_n$ is the n-mode tensor product [33] of a third-order tensor IL_G with the vector Q, with IL_G defined as:

$$IL_G^{kjg} = \Lambda_g^{kj} \tag{48}$$

with Λ_g defined by Eq. (6) for every girder g.

2.5.2. Comparing Matrix method and its 2D modification

In order to better understand the relation of the method proposed by Zhao et al. [9] and the Matrix Method in O'Brien et al. [19], one should take into account the formulation differences. Recalling Eq. (44), it is thus, possible to extract the constant Q as in:

$$\begin{aligned} IL_g &= ((AQ_g)^T (AQ_g))^{-1} (AQ_g)^T E_g Z_g \varepsilon_g^m \\ &= Q_g^{-2} (A^T A)^{-1} Q_g A^T E_g Z_g \varepsilon_g^m \\ &= Q_g^{-1} (A^T A)^{-1} A^T E_g Z_g \varepsilon_g^m. \end{aligned} \tag{49}$$

For the special case where the transverse distribution is constant along the bridge, this expression can be further simplified by writing:

$$Q_g = \frac{\varepsilon_g^m}{\varepsilon^m}, \tag{50}$$

where ε^m is the total strain over all girders obtained during one calibration event. Merging Eqs. (49) and (50):

$$IL_g = \left(\frac{\varepsilon_g^m}{\sum_{g=1}^{G} \varepsilon_g^m} \right)^{-1} (A^T A)^{-1} A^T E_g Z_g \varepsilon_g^m$$
$$= (A^T A)^{-1} A^T E_g Z_g \sum_{g=1}^{G} \varepsilon_g^m. \quad (51)$$

Therefore, if all girders have the same properties, namely E_g and Z_g, the Modified 2D method results in equal influence lines for each girder. Still under this condition, IL_g recovers the expression that would be obtained by employing the Matrix method. Thus, under such assumptions, both methods are equivalent in calibration.

In order to extend the analysis for the weighing procedure, the same assumption made in Eq. (50) could be incorporated into the theoretical bending moments expression, for any given scan:

$$\sum_{g=1}^{G} E_g Z_g \varepsilon_g^t = \sum_{g=1}^{G} W Q_g \Lambda_g. \quad (52)$$

Supposing that E_g and Z_g are equal for all girders, namely E and Z, it results that the influence lines IL_g would be the same, as previously discussed. Thus, Λ_g will also be the same, since it is a function of the influence lines of each girder. Calling Λ such a matrix of influence lines:

$$EZ \sum_{g=1}^{G} \varepsilon_g^t = W \Lambda \sum_{g=1}^{G} \left(\frac{\varepsilon_g^m}{\varepsilon^m} \right) \quad (53)$$

$$\sum_{g=1}^{G} E_g Z_g \varepsilon_g^t = W \Lambda. \quad (54)$$

Thus, the predicted moments for Matrix method and modified 2D Moses are the same, in this case. Therefore, one can conclude that, under the hypotheses of constant weight distribution and same mechanical properties of each girder, the weighing procedure also recovers the same solution found when applying the Matrix method, becoming independent of the distribution parameters.

2.6. Other approaches found in the literature

Regarding the methods that are focused in this paper, it is worth to point out that there are some proposed methodologies that address the same problem, however with characteristics that prevent a suitable comparison. In what follows, some of them are summarized and such aspects are discussed.

An approach to construct a more realistic influence line was proposed by Zhao et al. [34]. Their research intended to overcome the limitations of the theoretical influence line used by Moses in his first work. The bridge was modeled with semi-rigid connections and horizontal springs as boundary conditions. Moreover, it was included in the formulation the transverse load distribution, as proposed by Zhao et al. [9]. To completely define the model, it was necessary to estimate the values of some stiffness coefficients. In order to find these values, the author performed a trial and error procedure comparing measured and modeled values. Two algorithms were proposed: semi-rigid approach, adjusting end moments and semi-rigid approach, using moments of the whole bridge. Such methods were compared with Moses, employing the theoretical influence line. The experimental procedure used two trucks to calibrate and validate the method. The results showed that both proposed approaches achieved better results, specially the second method, which reached the lowest error among all. However, the procedure for finding the stiffness parameters that define the model does not have a clear definition. Thus, as such analysis could be user-dependent, performed comparisons may be inconclusive.

Kim et al. [18] proposed an approach to weigh vehicles using deformation measures as inputs to neural networks, obtaining the weights of each axle as the output. The error for both gross vehicle weight (GVW) and weight by axle were considerably low, indicating that the proposed approach could be applied in real situations. Nevertheless, the training process needed numerous training examples, preferably containing vehicles with distinct number of axles, which is not available in most practical cases. The advantage of this method was that it could be applied in cases where the traditional approach have some difficulties, which is not the focus of the present work.

In the work of Helmi et al. [35] three weigh methods were compared utilizing data of a real bridge in Canada. The first two methods were developed by the authors and consisted in the creation of an equivalent uniform distributed load to represent the axle loads, considering the influence line of a simply supported beam. The authors tried to find the fraction of the bridge span, corresponding to the length of the equivalent distributed load, which causes the maximum moment in the bridge. Thus, GVW could be calculated as the ratio between the maximum moment and this length. Nevertheless, both of the authors' proposed methods performed worse than the third alternative tested, namely the Beta method from Ojio and Yamada [36]. This method used the area under the moment or strain curve to calculate GVW, where errors of less than 5% were observed. However, none of such methods is able to distinguish the weight contribution of each axle, which is a parameter of comparison in the present paper.

The work of Frøseth et al. [3] intended to overcome issues related to implementation complexity and computational cost through the realization that the response of the structure is the convolution of the influence line and the loading. Thus, instead using the well-established matrix method, the author suggested that the convolution could be performed in frequency domain, since the convolution integral transforms into an element-wise multiplication operation, which is very efficiently handled. The reported gains in computational time were, in general, of one order of magnitude, at least. Another advantage of viewing the problem under the proposed aspect, was that the matrices utilized in the least-squares approach in O'Brien et al. [11] were straightforward to generalize for arbitrary number of axles. It is worth to mention that it may be necessary to apply a Tikhonov regularization in order to perform the deconvolution. The reason is that the system solution could result in an ill-posed problem in the frequency domain, for example, when the passing vehicle has two axles with identical loads. The author concluded that the obtained influence line provides virtually identical results in comparison with the matrix method. Therefore, the main practical utility of this approach was not precision, but computational gains. As computational complexity is not addressed in the present paper, no further analyses are performed for this method.

3. Numerical investigation

In addition to the theoretical argument presented in Section 2, this study aims to evaluate the numerical performance of discussed methods. This is justified given the usual absence of comparison among methods in literature. Table 1 illustrates this matter on studies that shall be evaluated. In this table, each row presents the method name, the comparison form employed, the type of data gathered and the method's characteristic of obtaining either influence line or weight. It becomes clear that recent work on the field has not been taken into account.

In order to compare the methods in a set of different conditions, a parametric investigation is conducted. The main factors that may

Table 1
Literature method comparisons.

Method	Comparison	Data	IL	Weight
Matrix [19]	Measured/Predicted	Real	✓	–
MLE [8]	Matrix method	Real	✓	–
PBWIM [10]	Matrix method	Real	–	✓
Regularization [11]	Matrix method	Synthetic	–	✓
Modified 2D Moses [9]	Measured/Predicted	Real	✓	✓

influence the performance of B-WIM algorithms are simulated numerically and the trend in gross vehicle weight error is measured and presented as result.

3.1. Numerical simulations

Recalling, the methods evaluated are the Matrix method [19], maximum likelihood (MLE) [8], pBWIM [10], Regularization [11] and Modified 2D Moses [9]. The procedure employed for finding the corner of the L curve for the regularization approach consisted on minimizing the Euclidean distance between adjacent points, as suggested in [37]. This is done utilizing all the pairs (E_{norm}, F_{norm}) employed for plotting the L-curve.

Regarding computational effort, almost all methods show similar values, being negligible for simulation purposes. The only exception is the pBWIM method, since this method depends on an optimization procedure for finding the most likely weights. Thus, while other methods can perform the computation directly by solving a single linear system, pBWIM may need several similar solution steps. The computational effort is shown to be increased by some orders of magnitude, mainly when the number of axles increases. This issue is partially handled in this study by employing a modified optimization procedure than that proposed by O'Brien et al. [10], which employed a grid search. Nevertheless, the computational effort still remains as a drawback for this method.

The model applied to artificially simulate the bridge strains is based on approximating the bridge behavior by a simply supported Euler-Bernoulli beam model, employing systems of sprung masses to represent each axle. The whole description of numerical procedures employed is further discussed in Appendix A.

The influence of two main aspects are evaluated on gross vehicle weight prediction, namely, road pavement profile and bridge span. Three distinct road profiles are evaluated, with Power Spectral Density (PSD) amplitudes of zero (no roughness), 4 and 16, where roughness increases with the amplitude. Further details on the description of this model are given in the Appendix A. For the bridge span parameter, three cases are considered, with spans of 10, 20 and 30 meters. Thus, the combination of every case of road profile and bridge span results in 9 distinct cases. Furthermore, a Gaussian noise with signal to noise ratio of 20 is added to every signal, aiming to incorporate measurement errors due to other sources than pavement roughness. It is worth to mention that the values adopted for all these cases intended to reflect the recommendations of Jacob [38] for B-WIM sites, hence, reproducing practical cases of interest.

In order to better approximate simulations with the real in-service operation behavior, a total of 200 vehicles, with number of axles ranging from 2 to 9, are simulated. The procedure for generating vehicles is random, where the absolute value of a normally distributed random variable ($\theta \sim \mathcal{N}(0, 1)$), is sampled and applied to Eq. (55).

$$J = \min(1 + \lceil 3.5(\mathrm{abs}(\theta)) \rceil, 9). \tag{55}$$

where $\lceil . \rceil$ is the ceil function, abs(.) is absolute value and J is the number of axles of the generated vehicle.

The histogram of vehicles sampled by this procedure is presented in Fig. 2 to illustrate that lower weight vehicles are more frequently created, an approach that intended to simulate a usual real scenario.

After the definition of the number of axles of the vehicle, a vehicle type is randomly chosen, which defines the bounds on axle spacing, damping, stiffness and maximum allowable weight on each axle. A total of 16 vehicle types are applied in this study, which are defined in Appendix B, based on a classification often used in Brazil. Axles spacing, damping, stiffness and weights are uniformly sampled based on the previously defined limits. Since axles weights does not have a minimum defined, a value of 80% of the maximum allowable weight is adopted. Furthermore, the velocity is uniformly sampled from a random variable with 10 m/s and 25 m/s as lower and upper bounds,

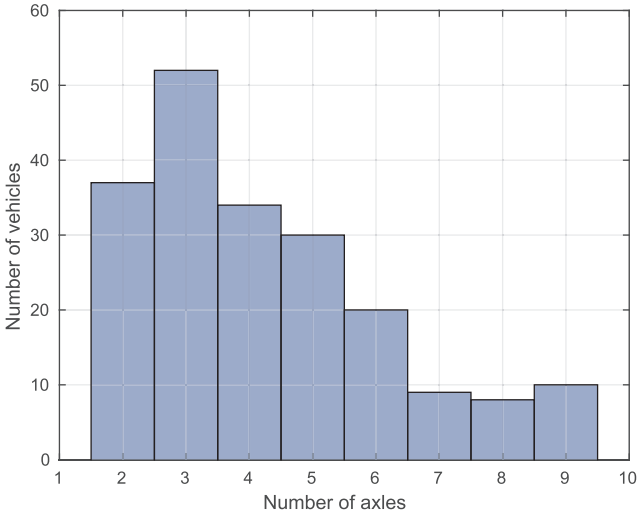

Fig. 2. Histogram of number of axles of vehicles created.

Table 2
Constant parameters.

Propertie	Value (Units)
Bridge modulus of elasticity	10^{10} (Pa)
Bridge damping coefficient	0.05 (–)
Bridge moment of inertia	0.5 (m^4)
Bridge mass per unit length	10^4 (kg/m)

respectively. The remaining parameters related to the bridge are taken as constants and are defined in Table 2. The same set of vehicles are applied to each one of the 9 cases.

A total of 40 runs of the vehicles 2C and 2S2, 20 for each of them, are applied to calibrate the system, simulating the real scenario where only a limited amount of calibration vehicles is available. For the calibration runs, vehicles speed are adopted accordingly with suggestions of Jacob [38]. Thus, 12 runs are executed with a mean velocity, adopted as 20 m/s here, 4 runs with 16 m/s and the remaining 4 runs with 24 m/s. After the calibration, all methods are applied to a test set comprised of the 200 runs which were previously generated.

3.2. Numerical results

The algorithms are evaluated in a set of different scenarios for assessing performance aspects and sensitivity of the methods. The comparison criterion consists of the mean absolute percentage error related to the known GVW. The results are shown in Fig. 3, as a function of roughness amplitude and bridge length. In order to facilitate the distinction among the performance of the methods, these values are also presented in Table 3, where some differences appear more evidently.

The simultaneous presentation of performance evolution with respect to both parameters, in Fig. 3 and Table 3, allow for quite interesting remarks. Firstly, all methods showed similar performance, mainly Matrix method, Regularization and Modified 2D Moses. The MLE method also shared the same trend, however, its performance surpassed the other methods when bridge span increases. This fact is observed independently of the roughness amplitude applied. Thus, although the difference is not so remarkable, the MLE method can be argued as the most accurate method for this data set.

On the other hand, pBWIM method showed similar performance for lower roughness amplitude, becoming worse than the others with the increase in this parameter. It is worth mentioning that the performance loss occurs in conjunction with a more computationally expensive prediction procedure.

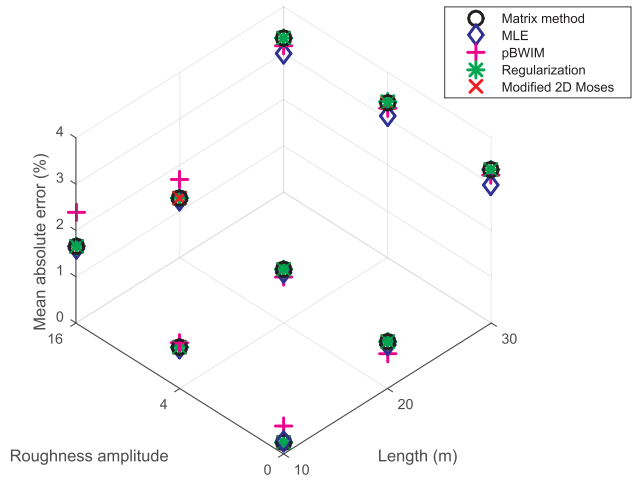

Fig. 3. Mean absolute error of each method as a function of bridge length and roughness amplitude.

Table 3
Mean absolute error for each method and case.

Amplitude	Length (m)	Matrix	MLE	pBWIM	Regularization	Modified 2D Moses
0	10	0.26	0.26	0.61	0.26	0.26
4	10	0.88	0.88	0.99	0.88	0.88
16	10	1.65	1.62	2.39	1.65	1.65
0	20	1.02	0.93	0.75	1.02	1.02
4	20	1.17	1.09	0.98	1.17	1.17
16	20	1.28	1.24	1.69	1.28	1.28
0	30	3.31	2.99	3.19	3.31	3.31
4	30	3.35	3.06	3.21	3.36	3.35
16	30	3.32	3.00	3.15	3.32	3.32

Table 4
Max of absolute difference between each method and the Matrix method.

Amplitude	Length (m)	MLE	pBWIM	Regularization	Modified 2D Moses
0	10	0.12	1.32	0.02	0.00
4	10	0.30	5.44	0.02	0.00
16	10	0.53	18.26	0.03	0.00
0	20	0.52	2.43	0.01	0.00
4	20	0.93	6.30	0.01	0.00
16	20	1.54	15.21	0.01	0.00
0	30	1.22	5.24	0.01	0.00
4	30	1.30	6.15	0.01	0.00
16	30	1.38	5.35	0.01	0.00

Since the whole bridge is simulated as a unique beam, it is already expected for Modified 2D Moses and Matrix method results to be numerically identical. Indeed, in all evaluated cases and runs, the results are exactly the same. However, Regularization also shows similar behavior, presenting only slight deviations from the trends in the Matrix method. Such aspects can be seen in Table 4, where the maximum deviation of each method with respect to the Matrix method is presented. One can conclude that, in the conditions of this analysis, the difference in performance among Matrix method and Regularization is not significant. The reason is that the parameters found were usually close to zero, which promotes solutions very close to the least squares in the Matrix method. Nevertheless, it does not mean that the regularization approach is not useful, however, in the examples, the application of the L-curve corner lead to similar results. Therefore, it did not have a large influence in the cases analyzed here.

In order to correctly analyze the method presented by Zhao et al. [9], it is necessary to take into account multiple beams in the bridge, which is addressed in the following sections.

When comparing the evolution of mean absolute error regarding bridge length and roughness amplitude separately, one can conclude that the first is more problematic. The difficulty of static methods in dealing with long span bridges is a fact already well known on B-WIM literature [38,18]. However, the comparison of variation of bridge length and roughness amplitude shows an interesting aspect. Analyzing the results, it is clear that bridge length has a higher impact on the overall result than the roughness amplitude, since the cases of smooth profile and 30 m bridge span easily surpass the error of the 10 m bridge span and roughness amplitude of 16.

It is interesting to notice that the increase in bridge length spreads the effect of roughness in the prediction accuracy. Thus, the result is more sensible to the road pavement profile for short span bridges. The opposite is not true, in other words, independently of the roughness amplitude, the increase in bridge length decreases the accuracy of weight prediction.

3.3. Multiple beams analysis

Given that Modified 2D Moses and Matrix method resulted in rigorously the same predictions in previous analyses, it becomes necessary simulating cases where the bridge response is modeled considering multiple beams. In this section, the bridge structure is comprised of 3 distinct beams, where the simulation details are also referred to Appendix A. Moreover, the same vehicles and properties previously defined are adopted in this section. Three distinct cases of transverse distribution (Q) are considered, defined by Table 5.

Since pBWIM, MLE and Regularization methods do not make any assumption regarding transverse distribution of loads, their evaluation for this new case should not bring any new insight. Thus, only as a comparison criterion, the Matrix method is jointly evaluated with Modified 2D Moses. As a result of this analysis, Figs. 4–6 present the influence of roughness amplitude and transverse distribution case for each bridge span.

In all cases, Modified 2D Moses performed equally or worse than Matrix method. In the case of low roughness amplitude, both methods could be argued as similar. When roughness amplitude increases, otherwise, there is a trend for the Modified 2D Moses method to present higher errors, for all analyzed bridge spans. Such performance gap is specially remarkable in the 10 m bridge. This last statement is in agreement with the previous section, where the effect of road profile showed higher impact for short span bridge cases.

One possible explanation for the performance gap can be seen in Fig. 7. It shows the influence of the error in approximating Q (measured as the mean of Euclidean distance among predicted and real Q values) and the percentage difference between the results of the two methods. This figure makes clear that the accuracy in Q estimate is directly related to the difference in performance when compared with the Matrix method. Therefore, if transverse distribution factors can be accurately predicted, Modified 2D Moses approximates Matrix method performance. This fact is in accordance with Section 2.5.2, since Q values are kept constant in the simulation. On the other hand, the increase in difference of such factors also increases the likelihood that weight prediction is corrupted.

Table 5
Load distribution factors for each beam (%).

Case	Beam 1	Beam 2	Beam 3
Q1	33.3	33.3	33.3
Q2	20.0	40.0	40.0
Q3	25.0	50.0	25.0

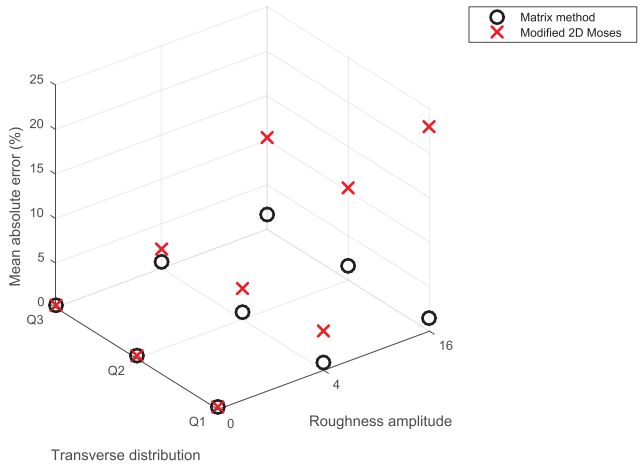

Fig. 4. Comparison between Matrix method and Zhao for bridge span of 10 m.

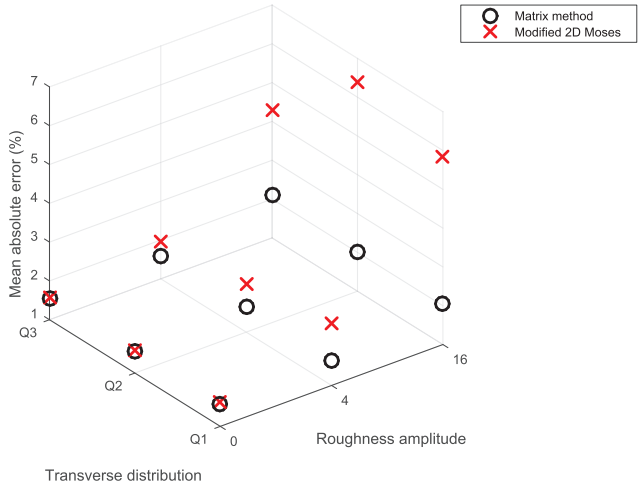

Fig. 5. Comparison between Matrix method and Modified 2D Moses for bridge span of 20 m.

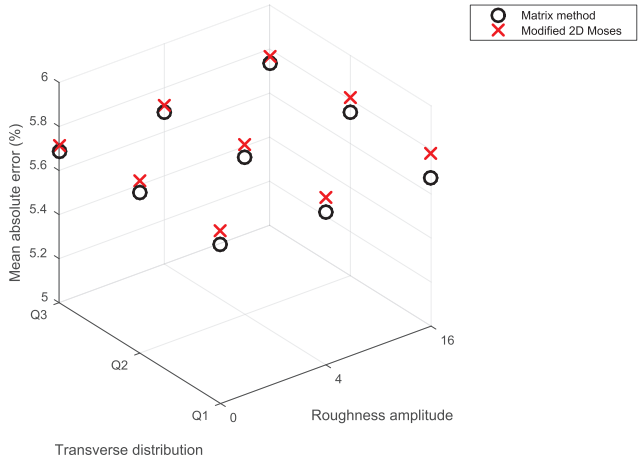

Fig. 6. Comparison between Matrix method and Modified 2D Moses for bridge span of 30 m.

4. Field-testing

In order to compare the different methods presented in Section 3.2 on a real-world setting, data from a bridge located in the city of Uruaçu, Brazil, is employed. The main aspects regarding such bridge and the calibration procedure are described in what follows.

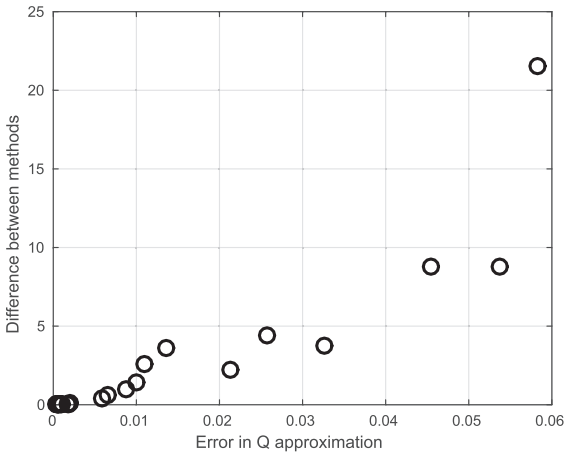

Fig. 7. Influence of error in transverse distribution factor on the difference between methods.

Fig. 8. Itinguijada bridge.

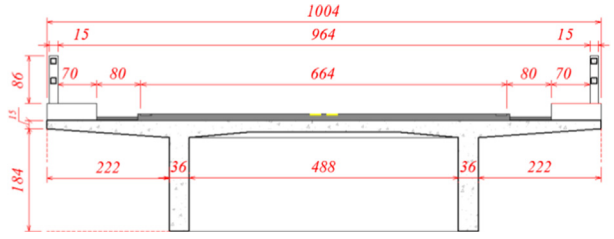

Fig. 9. Mid-span cross section dimensions.

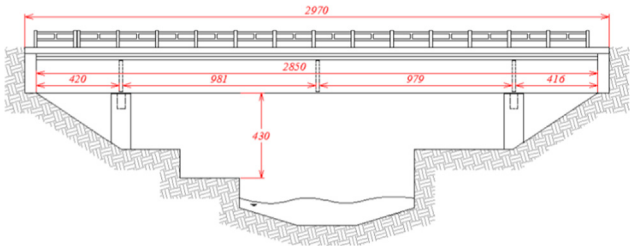

Fig. 10. Lateral view dimensions.

Table 6
Axle weights and spacing for Itinguijada bridge.

	Axle weight (kN)					Axle spacing (m)			
	Axle 1	Axle 2	Axle 3	Axle 4	Axle 5	d_{12}	d_{23}	d_{34}	d_{45}
3 axle vehicle	67.7	146.2	125.5	–	–	4.78	1.28	–	–
5 axle vehicle	73.6	138.3	130.4	108.9	90.3	3.57	5.59	1.26	1.23

Table 7
Mean absolute error.

	Matrix method	MLE	pBWIM	Regularization	Modified 2D Moses
GVW (%)	4.47	4.08	4.91	4.40	4.41
Single axle (%)	17.79	15.26	36.46	15.35	16.91
Group of axles (%)	6.62	5.38	5.78	6.22	6.52

Table 8
Difference between each approach and the Matrix method.

	MLE	pBWIM	Regularization	Modified 2D Moses
Mean (%)	1.2101	4.2554	0.3860	0.1526
Std (%)	0.6351	3.6975	0.2901	0.1153
Maximum (%)	2.5673	16.6928	1.2900	0.6864

4.1. Bridge and vehicle description

The Itinguijada bridge, shown in Fig. 8, is comprised by two girders and five cross beams, with a total length of 29.0 m. Figs. 9 and 10 show the main dimensions of the cross section and the lateral view, respectively. One FAD sensor is installed in the mid-span of the bridge, while the other is spaced 4 meters longitudinally from the first. Two strain sensors were attached to each girder, at the mid-span.

Two trucks, with three and five axles, are used for calibrating and evaluating the system performance. Several runs with each of these vehicles are conducted, totaling at least 10 runs per truck and lane. The axle spacing and weight distribution for the calibration vehicles are shown in Table 6.

4.2. Numerical results

In this section, following what is done in practice, as reported in Lydon [5] and Yu et al. [1], one influence line is constructed for each lane. The analyses are based on prediction for three distinct quantities, defined by Jacob [38]: GVW, single axle and group of axles. The mean absolute error of such quantities for each method on the whole data set is presented in Table 7.

All methods showed higher errors for single axle prediction when compared to the group counterparts, which is in accordance with most studies in this subject, as in Zhao et al. [9] and O'Brien et al. [11]. The prediction for GVW and group of axles weight showed reasonable results, with mean absolute errors always smaller than 7%. However, single axle prediction did not present the same level of performance, achieving values as high as 36% for pBWIM method.

MLE reached the best results, independently of the quantity being measured. However, for almost all methods and quantities measured, the mean absolute errors reported remained at a quite similar level. Since all methods disregarded dynamic effects, it is expected that the higher such effects are, the lower the suitability of all approaches are. As in this bridge the dynamic behavior is not remarkable, the results for MLE suggests that this method should perform better in cases where the model seems to be more suitable.

The similarity of measured errors previously discussed justify a more detailed analysis on it. Table 8 focus on this statement, based on the absolute difference in GVW, for each event, between all methods and the Matrix method, taken as reference here. The parameters presented are the mean, standard deviation and maximum value of the absolute difference.

From the five analyzed methods, two can be seen as almost identical to the Matrix method. The first of them is the Regularization method, whose maximum difference in GVW for all events does not surpass 1.29 %. This lack of difference, as already discussed in Section 3, is caused by small regularization parameters obtained from the application of L-curve method. The second method quite similar to the Matrix method is Modified 2D Moses, in which maximum difference did not reached 1%. As already discussed, all girders have the same mechanical properties, which remain constant along the span. Thus, it is possible that the contribution factor Q_g resulting for each girder and event be approximately a constant value. As presented in Section 2.5.2, in such a case it is already expected for results of Matrix method and modified 2D Moses to be similar.

The remaining two methods, MLE and pBWIM, showed more distinct values, rendering them as alternative approaches for the Matrix method. Observing these three methods by a probabilistic point of view, these differences are remarked. The Matrix method is based on least squares, which assumes that errors are uncorrelated, normally distributed and with the same variance, using all the measurements of one event as the realization of only one normal random variable. The MLE method also applies the least squares approach, however now considering a multivariate normal distribution whose variables are moments measured in each ordinate, independently of the other ordinates. The pBWIM relaxes the assumption of equal variance, allowing for each ordinate to have a standard deviation estimated by the value of each influence line previously calculated from calibration events. Therefore, in some cases, namely when the data from both distinct events and the whole bridge have the same normal distribution, all methods should

Table 9
Vehicle types employed in the study.

Vehicle Class	Axles
2C	2
3C	3
4CD, 2S2	4
3I2, 2S3, 3S2	5
2R4, 3S3, 3D3, 3N3	6
3D4, 3N4	7
3D5	8
3M6, 3Q6	9

Table 10
Mean values of stiffness and damping coefficients for each kind of axle

Axle type	Stiffness (N/m)	Damping (Ns/m)
Rear	1,000,000	10,000
Front	400,000	10,000
Semi trailer	750,000	10,000

present virtually the same results. However, considering the real-world examples presented, this is not the case in practical applications.

One could say that pBWIM should achieve the best result, since this method has the least restrictive formulation. However, one must realize that this can only occur if the assumptions are met, and this is not the case for the pBWIM formulation, as demonstrated in Section 2.3.2. It could be observed that this method assumes uncorrelated error moments. Yet, the formulation based on uncertainties in influence line will necessarily result in banded correlation of the resulting moments random variable, violating this assumption.

5. Further remarks

Among five tested methods, three of them showed almost identical results for all events evaluated, namely, the Matrix method, Regularization and Modified 2D Moses. Although the pBWIM method could be argued as an alternative approach for weight prediction, both theoretical and practical results are not promising. Comparing MLE and Matrix method, the results for the simulated runs were very similar, however with MLE being slightly better. Furthermore, when field-testing was conducted, MLE approach showed even better performance. These points, together with its more suitable statistical background, indicates that MLE is the most promising method evaluated in the present study. Some suggestions for improving these methods are included in the following.

The formulation employed for Regularization leads to a solution that recovers only weights associated with each axle. However, it is possible that the regularization approach can have improved results when trying to recover the whole impulse vector, as more information about its characteristics may be incorporated and enforced by the regularization procedure. Furthermore, it may be worth to employ different regularization procedures instead of Tikhonov, such as Lasso, which uses the L1 norm instead of the usual L2 [39]. As a further step, the non-negativity of the vector can be enforced as in the work of Hummelsheim [40].

Discussing specifically the pBWIM method, it could be concluded that an assumption made in the approach formulation is conceptually violated. Thus, it is useful to change such a methodology to account for a covariance matrix that is not diagonal. Furthermore, the procedure suggested to find the most likely weights in the original paper is quite-time consuming. Thus, applying an optimization procedure is necessary for achieving a reasonable computational cost.

The procedures applied are clearly divided in two steps: building an influence line and weighing the vehicles. From this perspective, one could easily apply distinct methods for each step. For instance, MLE could address the former and regularization the latter. Since it was not the focus of this work, coupling methods was not evaluated. However, it has potential to improve the accuracy of predicted axle weights.

Overall, it becomes clear that the main point that should be addressed is the incorporation of additional knowledge to the model. One aspect is related to dynamic effects. The results could be improved by a more suitable consideration on the dynamic behavior of the vehicle-bridge system model. A second aspect is related to the form of the solution. The knowledge that a vehicle is modeled by point loads on each axle imposes constraints on the form of the impulse vector and the sign of the resulting weights. Nevertheless, relaxing assumptions that over-constrain the model, such as the correctness of axle spacing measurement, may improve flexibility and robustness to the methods.

For all evaluated methods, the weighing procedure disregarded some prior information that could lead to more reliable estimates. As examples, one could cite the non-negativity of weights and the trend for axle weights having values at the same order of magnitude. As discussed previously, a Bayesian approach could be employed in such a case, using these prior information to create improved estimators for axle weights.

When observing methods by the statistical point of view, the assumptions implicitly made in the development of such formulations arose in a more clear fashion. Thus, the possibilities of relaxing some of those assumptions could be seen as a good initial point for the development of new methods. Furthermore, by knowing in advance which statistical assumption was made, it becomes possible to easily predict for which real cases the new methods could perform better. As an example, allowing errors to be correlated should perform better in problems where the model fits poorly, since missing information on formulation could be seen as correlated errors. Thus, enabling the model to allow correlated error is an alternative to address the dynamic effects.

The comparison criterion of the evaluated methods was done without a clear performance threshold. Thus, although it is possible to verify which method is best in the tested cases, nothing can be said about robustness or suitability of overall results. Therefore, it motivates the development of a methodology for extracting more useful information from such results, mainly regarding robustness in practical applications.

6. Concluding remarks

This work presented a comparative study regarding some methods applied in B-WIM systems to derive the bridge influence line and predict vehicle weights. In order to fairly compare the analyzed methods, only those which do not explicitly address the dynamic behavior of the vehicle-bridge system were considered. Furthermore, the methods were interpreted from a statistical point of view, where their assumptions were highlighted, remarking their theoretical differences.

In addition to the theoretical comparisons, the methods were implemented and numerically compared, addressing the lack of comparisons found in literature. In order to assess the similarity or the advantage of a method compared to the others, synthetically generated and real data were considered. Furthermore, the influence of some main factors that affect B-WIM systems were evaluated in simulated analyses, such as road profile and bridge length.

The analysis using simulated data showed that the increase in bridge length had more impact in corrupting the overall results than the roughness amplitude. The influence of road profile increased when decreasing the bridge span. When analyzing the performance of the methods, results indicated that pBWIM and Modified 2D Moses were surpassed by the other approaches. Indeed, pBWIM usually provided worse weight estimation performance, together with a considerably higher computational cost. Modified 2D Moses was, for all analyzed cases, equal or worse than Matrix method. The remaining methods, MLE, Matrix method and Regularization, presented very similar results, with MLE being slightly better. The results regarding real data followed the trend already observed in numerical simulation, however with MLE showing superior performance. Thus, from both theoretical and

practical perspectives, the MLE could be argued as the most promising method evaluated in this study.

Overall, the reformulation and reinterpretation of methods under a common statistical point of view allowed a better understanding of the underlying assumptions and theoretical hypothesis. This fact enabled a better comparison among methods and generated an opportunity for further improvements. For example, developing novel methods by relaxing the model statistical assumptions or applying a Bayesian approach to better account for prior information.

Acknowledgements

This study was financed in part by the Coordenação de Aperfeiçoamento de Pessoal de Nível Superior - Brasil (CAPES) – Finance Code 001 and the Transport Infrastructure National Department (DNIT).

Appendix A. Sprung-mass simulation

In the present study, the simulations are based on the works of Biggs [41], Yang et al. [42] and Yang and Lin [43]. The resulting dataset is available online [44]. The dynamic behavior of the bridge is modeled supposing a simply supported Euler Bernoulli beam model, under a set of moving sprung-masses. In this approach, each sprung-mass system represents one vehicle axle. Modal decomposition is performed for the equation of motion of the bridge, resulting in Eq. (56):

$$\ddot{q}_i + 2\xi_i\omega_i\dot{q}_i + \omega_i^2 q_i = \sum_{j=1}^{N} \frac{2P_j}{\bar{m}L}\sin\frac{i\pi Vt}{L}, \tag{56}$$

where N is the number of axles, q_i, ω_i and ξ_i are the modal coordinates, natural frequency and damping of the i mode, respectively. Furthermore, dotted variables represent the derivative with respect to time, P_j is the load of the j axle, V the speed of the vehicle, L is the length of the bridge and $\bar{m}$ is the mass per unit length of the bridge.

The equations of motion for each sprung-mass system is given by Eq. (57):

$$M_{vj}\ddot{z}_j + C_{vj}\dot{z}_j + K_{vj}z_j = K_{vj}(u + y)|_{x=Vt} + C_{vj}(\dot{u} + Vy')|_{x=Vt}, \tag{57}$$

where M_{vj}, C_{vj} and K_{vj} are the mass, damping and stiffness of axle j. Furthermore, u represents the bridge vertical displacement, z_j is the vertical position of the j axle, y is the pavement elevation ordinate and a prime denotes the derivative with respect to x.

Both bridge displacement and its first derivative could be computed directly with the modal coordinates and mode shapes of the simply supported beams:

$$u = \sum_{j=1}^{m} \sin\left(\frac{j\pi x}{L}\right)q_i, \tag{58}$$

$$\dot{u} = \sum_{j=1}^{m} \sin\left(\frac{j\pi x}{L}\right)\dot{q}_i, \tag{59}$$

where m is the number of modes applied, which is equal to 5 in all simulations.

The simulation of pavement roughness applied here is a common approach in studies in the same subject [45,46,16]. The ordinates of the pavement irregularities are modeled as a random process, with a specific power spectral density function (PSD):

$$\Phi(\Omega) = \Phi(\Omega_0)\left(\frac{\Omega}{\Omega_0}\right)^{-2}, \tag{60}$$

where $\Phi(\Omega_0)$ is the amplitude coefficient, analyzed in previous sections, measured in (10^{-6} m^3/cycle) and Ω_0 is a reference spatial frequency. Thus, the road profile is generated by sampling from this PSD, using the method of superposition of harmonics [47]:

$$y(x) = \sum_{i=1}^{n\Omega} \sqrt{2\Delta\Omega\Phi(\omega_i)}\cos(2\pi\Omega_i x - \phi_i) \tag{61}$$

where $y(x)$ is the generated road vertical profile, ϕ_i is a random uniform phase angle between 0 and 2π, $\Delta\Omega$ is a constant increment, $n\Omega$ is the total number of frequency increments in the interval and Ω_i is a frequency uniformly distributed in the range of Ω_{min} and Ω_{max}. The parameters adopted are $\Omega_0 = 0.01$ cycle/m, $\Omega_{min} = 0.001$ cycle/m, $\Omega_{max} = 4$ cycle/m and $\Delta\Omega = 0.001$ cycle/m.

It is worth to mention that for each run a distinct road profile is generated, since in the practical scenario lateral deviations occur. Moreover, a moving average with total size of 30 cm is employed to approximate the real contact between tire and pavement [46].

The interaction between bridge and vehicle clearly appears in Eq. (57), by means of the displacement term related to the beam at the current axle position. Moreover, such interaction also occurs in Eq. (56), due to the P_j term. This relation is remarked in Eq. (62):

$$P_j = p_j\delta(x - Vt)\left(H(t - t_j) - H\left(t - t_j - \frac{L}{V}\right)\right), \tag{62}$$

$$p_j = -M_{vj}g + K_{vj}(z - (u + y)|_{x=Vt}) + C_{vj}(\dot{z} - (\dot{u} + Vy')|_{x=Vt}), \tag{63}$$

with $\delta()$ and $H()$ representing the Dirac delta and Heaviside functions, respectively. Moreover, g is the acceleration of gravity and t_j is the time that the j axle arrives the bridge.

The equations of motion are solved independently, by a decoupled approach. Both bridge and vehicle equations are solved numerically by applying the Newmark-β method, with 1400 time steps. The time window begins when the first vehicle axle enters the bridge and ends when the last axle leaves it. The problem is solved iteratively, since the interaction force in the bridge-vehicle system changes with the displacement of both beam and sprung mass. An initial guess of interaction force is given to the beam equations, where the beam displacement is calculated. Such a displacement is then enforced to the vehicle model and a new interaction force is calculated. This procedure continues until the change in the

interaction force reaches a small tolerance (10^{-5}). Usually such procedure converges rapidly, within 5 iterations. The midspan strains (s), which are the main output of simulation, are also updated with this interaction. Adopting, without loss of generality, a unit vertical distance from the neutral axis, and utilizing the fact that strains are related with the second derivative of displacement with respect to x, the strains can be written as:

$$s = -\sum_{i=1}^{m} \left(\frac{i\pi}{L}\right)^2 q_i \sin\left(\frac{i\pi}{2}\right). \tag{64}$$

For the case of multiple beams, a transverse distribution factor (Q) is provided and applied to divide the axle loads for each beam. Thus, each beam is simulated independently.

In order to simulate the inherent imperfections of the measured signal due to all possible aspects in the measurement field, noise is applied to the simulated response. The noise applied consists of a white Gaussian random noise, with a constant signal to noise ratio of 20.

Appendix B. Vehicle types

The vehicles employed are based on the brazilian's traffic and infrastructure department report [48]. As some classes have only a lower bound for axle spacing, the upper bound for such cases is defined as 5 meters, since this is necessary for generating vehicles in a uniform distribution. Table 9 presents all types of vehicle employed as well as their number of axles. In order to allow a more concise presentation, axle spacing and weight of each employed truck are omitted. For assessing such values, the reader is referred to DNIT IPR 723 [48].

On the other hand, damping and stiffness coefficients still need to be defined. In this study, each vehicle have a specific coefficient related to each axle, which is a random variable uniformly distributed around a mean value, presented in Table 10. This distribution have bounds of 0.5 and 1.5 times this mean value, which is adopted based on Fancher [49] and Nosseir et al. [50]. It is worth to cite that such mean values differ accordingly with the type of axle, namely: rear, front or semi trailer axle.

Appendix C. Supplementary material

Supplementary data associated with this article can be found, in the online version, at https://doi.org/10.1016/j.engstruct.2019.109463.

References

[1] Yu Yang, Cai CS, Deng Lu. Nothing-on-road bridge weigh-in-motion considering the transverse position of the vehicle. Struct Infrastruct Eng 2018;14(8):1108–22.
[2] Lansdell Andrew, Song Wei, Dixon Brandon. Development and testing of a bridge weigh-in-motion method considering nonconstant vehicle speed. Eng Struct 2017;152:709–26.
[3] Frøseth Gunnstein T, Rønnquist Anders, Cantero Daniel, Øiseth Ole. Influence line extraction by deconvolution in the frequency domain. Comput Struct 2017;189:21–30. https://doi.org/10.1016/j.compstruc.2017.04.014. ISSN 0045-7949.
[4] Moses Fred. Weigh-in-motion system using instrumented bridges. J Transp Eng 1979;105(3).
[5] Lydon Myra, Taylor Su E, Robinson Desmond, Mufti A, Brien EJO. Recent developments in bridge weigh in motion (b-wim). J Civ Struct Health Monit 2016;6(1):69–81.
[6] Yu Yang, Cai CS, Deng Lu. State-of-the-art review on bridge weigh-in-motion technology. Adv Struct Eng 2016;19(9):1514–30.
[7] Žnidarič Aleš, Kalin Jan, Kreslin Maja. Improved accuracy and robustness of bridge weigh-in-motion systems. Struct Infrastruct Eng 2018;14(4):412–24.
[8] Ieng Sio-Song. Bridge influence line estimation for bridge weigh-in-motion system. J Comput Civ Eng 2015;29(1):06014006. https://doi.org/10.1061/(ASCE)CP.1943-5487.0000384.
[9] Zhao Hua, Uddin Nasim, O'Brien Eugene J, Shao Xudong, Zhu Ping. Identification of vehicular axle weights with a bridge weigh-in-motion system considering transverse distribution of wheel loads. J Bridge Eng 2014;19(3):04013008. https://doi.org/10.1061/(ASCE)BE.1943-5592.0000533.
[10] O'Brien Eugene J, Zhang Longwei, Zhao Hua, Hajializadeh Donya. Probabilistic bridge weigh-in-motion. Can J Civ Eng 2018;45(8):667–75. https://doi.org/10.1139/cjce-2017-0508.
[11] O'Brien Eugene J, Rowley Cillian W, Gonzalez Arturo, Green Mark F. A regularised solution to the bridge weigh-in-motion equations. Int J Heavy Veh Syst 2009;16(3):310–27. https://doi.org/10.1504/IJHVS.2009.027135.
[12] Wang Ning-Bo, He Li-Xiang, Ren Wei-Xin, Huang Tian-Li. Extraction of influence line through a fitting method from bridge dynamic response induced by a passing vehicle. Eng Struct 2017;151:648–64.
[13] Wang Yi, Wei-Lian Qu. Moving train loads identification on a continuous steel truss girder by using dynamic displacement influence line method. Int J Steel Struct 2011;11(2):109–15.
[14] Dowling Jason OBrien Eugene J, González Arturo. Adaptation of cross entropy optimisation to a dynamic bridge wim calibration problem. Eng Struct 2012;44:13–22. doi: https://doi.org/10.1016/j.engstruct.2012.05.047. http://www.sciencedirect.com/science/article/pii/S0141029612002908. ISSN 0141-0296.
[15] Deng Lu, Cai CS. Identification of dynamic vehicular axle loads: theory and simulations. J Vib Control 2010;16(14):2167–94.
[16] Wang Haoqi, Nagayama Tomonori, Zhao Boyu, Di Su. Identification of moving vehicle parameters using bridge responses and estimated bridge pavement roughness. Eng Struct 2017;153:57–70.
[17] Richardson Jim, Jones Steven, Brown Alan, O'Brien Eugene J, Hajializadeh Donya. On the use of bridge weigh-in-motion for overweight truck enforcement. Int J Heavy Veh Syst 2014;21(2):83–104.
[18] Kim Sungkon, Lee Jungwhee, Park Min-Seok, Jo Byung-Wan. Vehicle signal analysis using artificial neural networks for a bridge weigh-in-motion system. Sensors (Basel) 2009;9(10).
[19] O'Brien Eugene J, Quilligan Michael, Karoumi Raid. Calculating an influence line from direct measurements. Bridge Eng Proc Inst Civ Eng 2006;159(BE1):31–4.
[20] Aster Richard C, Borchers Brian, Thurber Clifford H. Parameter estimation and inverse problems vol. 90. Academic Press; 2011.
[21] Washington Simon P, Karlaftis Matthew G, Mannering Fred. Statistical and econometric methods for transportation data analysis. Chapman and Hall/CRC; 2010.
[22] Chatterjee Samprit, Hadi Ali S. Regression analysis by example. John Wiley & Sons; 2015.
[23] Hansen P. Rank-deficient and discrete Ill-posed problems. Soc Ind Appl Math 1998. https://doi.org/10.1137/1.9780898719697.
[24] Golub Gene H, Heath Michael, Wahba Grace. Generalized cross-validation as a method for choosing a good ridge parameter. Technometrics 1979;21(2):215–23.
[25] Hoerl Arthur E, Kennard Robert W. Ridge regression: biased estimation for non-orthogonal problems. Technometrics 1970;12(1):55–67.
[26] Hansen Per Christian. Analysis of discrete ill-posed problems by means of the l-curve. SIAM Rev 1992;34(4):561–80.
[27] Hansen Per Christian, O'Leary Dianne Prost. The use of the l-curve in the regularization of discrete ill-posed problems. SIAM J Sci Comput 1993;14(6):1487–503.
[28] Longina Castellanos J, Gómez Susana, Guerra Valia. The triangle method for finding the corner of the l-curve. Appl Numer Math 2002;43(4):359–73.
[29] Hansen Per Christian. Toke Koldborg Jensen, and Giuseppe Rodriguez. An adaptive pruning algorithm for the discrete l-curve criterion. J Comput Appl Math 2007;198(2):483–92.
[30] Congdon Peter. Bayesian statistical modelling vol. 704. John Wiley & Sons; 2007.
[31] Tarantola Albert. Inverse problem theory and methods for model parameter estimation vol. 89. Siam; 2005.
[32] Kaipio Jari, Somersalo Erkki. Statistical and computational inverse problems vol. 160. Springer Science & Business Media; 2005.
[33] Kolda Tamara G, Bader Brett W. Tensor decompositions and applications. SIAM Rev 2009;51(3):455–500.
[34] Zhao Zhisong, Uddin Nasim, O'Brien Eugene J. Bridge weigh-in-motion algorithms based on the field calibrated simulation model. J Infrastruct Syst 2017;23(1):04016021. https://doi.org/10.1061/(ASCE)IS.1943-555X.0000308.
[35] Helmi Karim, Bakht Baidar, Mufti Aftab. Accurate measurements of gross vehicle weight through bridge weigh-in-motion: a case study. J Civ Struct Health Monit 2014;4(3):195–208.
[36] Ojio T, Yamada K. Bridge weigh-in-motion systems using stringers of plate girder bridges. Third international conference on weigh-in-motion (ICWIM3). Ames: Iowa State University; 2002.
[37] Frasso Gianluca, Eilers PH. Smoothing parameter selection using the l-curve. In: 27th international workshop on statistical modelling, Prague, Czech Republic, 2012, Proceedings; 2012.
[38] Jacob B. Cost 323 weigh in motion of road vehicles. Final report, appendix 1

European wim specification; 1999.
[39] Tibshirani Robert. Regression shrinkage and selection via the lasso. J Roy Stat Soc Ser B (Methodological) 1996:267–88.
[40] Hummelsheim S. Lasso and equivalent quadratic penalized models. ArXiv e-prints; 2014.
[41] Biggs John M. Introduction to structural dynamics. McGraw-Hill College; 1964.
[42] Yeong-Bin Yang JD, Yau Zhongda Yao, Wu YS. Vehicle-bridge interaction dynamics: with applications to high-speed railways. World Scientific; 2004.
[43] Yang YB, Lin CW. Vehicle–bridge interaction dynamics and potential applications. J Sound Vib 2005;284(1–2):205–26.
[44] Gonçalves Matheus Silva, Carraro Felipe, Lopez Rafael Holdorf. Vehicle-bridge dynamics simulation. Mendeley Data; 2019. URL https://doi.org/10.17632/kt48wf5vjz.1.
[45] Múčka Peter. Simulated road profiles according to iso 8608 in vibration analysis. J Test Eval 2017;46(1):1–14.
[46] Miguel Leandro FF, Lopez Rafael H, Torii André J, Miguel Letícia FF, Beck André T. Robust design optimization of tmds in vehicle–bridge coupled vibration problems. Eng Struct 2016;126:703–11.
[47] Dharankar Chandrashekhar S, Hada Mahesh Kumar, Chandel Sunil. Numerical generation of road profile through spectral description for simulation of vehicle suspension. J Braz Soc Mech Sci Eng 2017;39(6):1957–67.
[48] DNIT IPR 723. Manual de estudos de tráfego. Departamento Nacional de Infraestrutura e Transportes, Rio de Janeiro, Brazil; 2006.
[49] Fancher Paul S. A factbook of the mechanical properties of the components for single-unit and articulated heavy trucks. Phase i. Final report; 1986.
[50] Nosseir TA, El-Gindy M, El-Saied FA. Tire radial properties. J Periodica Polytech Transp Eng 1982:21–8.